nature medicine

Using siRNA in prophylactic and therapeutic regimens against SARS coronavirus in Rhesus macaque

Bao-jian Li[1,2,7], Qingquan Tang[3,7], Du Cheng[2,7], Chuan Qin[4,7], Frank Y Xie[2,3], Qiang Wei[4], Jun Xu[3], Yijia Liu[3], Bo-jian Zheng[5], Martin C Woodle[3], Nanshan Zhong[6] & Patrick Y Lu[3]

Development of therapeutic agents for severe acute respiratory syndrome (SARS) viral infection using short interfering RNA (siRNA) inhibitors exemplifies a powerful new means to combat emerging infectious diseases. Potent siRNA inhibitors of SARS coronavirus (SCV) *in vitro* were further evaluated for efficacy and safety in a rhesus macaque (*Macaca mulatta*) SARS model using clinically viable delivery while comparing three dosing regimens. Observations of SARS-like symptoms, measurements of SCV RNA presence and lung histopathology and immunohistochemistry consistently showed siRNA-mediated anti-SARS efficacy by either prophylactic or therapeutic regimens. The siRNAs used provided relief from SCV infection–induced fever, diminished SCV viral levels and reduced acute diffuse alveoli damage. The 10–40 mg/kg accumulated dosages of siRNA did not show any sign of siRNA-induced toxicity. These results suggest that a clinical investigation is warranted and illustrate the prospects for siRNA to enable a massive reduction in development time for new targeted therapeutic agents.

The outbreak of SARS has posed an urgent need to understand its disease pathogenesis[1–3] and the biology of its causative agent, now identified as SCV[4–8]. Individuals with SARS usually develop a high fever followed by severe clinical symptoms including acute respiratory distress syndrome with a diffuse alveolar damage (DAD) at autopsy[2,4,9]. The containment of SARS has been achieved largely through traditional quarantine and sanitation measures[9,10]. Because SARS is a newly emerging disease, a safe and effective vaccine is not yet available[11], although some candidate vaccines have been advanced to monkey models and clinical testing[12–15]. To treat individuals with SARS, combinations of existing drugs, including ribavirin, antibiotics, anti-inflammatory steroids and immune stimulators, have achieved some clinical success[16–18]. Many ongoing efforts to develop SARS-specific drugs, such as screening of small-molecule inhibitors and current biologic approaches, will clarify the strengths and weaknesses of each approach, based on the ultimate success rate and the time and cost incurred[19,20].

The identification of SCV as the causative pathogen of SARS was achieved mainly by demonstration that exposure of cynomolgus macaques to SCV resulted in symptoms similar to those of individuals with SARS[1,2]. Meanwhile, development of macaque models became important not only for understanding SARS pathogenesis but also for evaluation of potential vaccines and therapeutics[11–13,16,19,20]. Recently, a Rhesus macaque SARS model was established with intranasal instillation of SCV strain PUMC01, showing many elements of pathology similar to those of individuals with SARS[21,22]. The pathogenesis includes elevated body temperature, low appetite and acute DAD clearly visible at 7 d after infection (d.p.i.), but with somewhat worse severity than other macaque SARS models[19,20], offering an ideal model for evaluation of therapeutic candidates.

The search for developing antiviral agents directly from viral genome sequences has led to short interfering RNA (siRNA), the mediator of a sequence-selective inhibition known as RNA interference (RNAi)[23]. We reported a screen of 48 siRNA candidates targeting elements throughout the entire SCV genome and identified several siRNAs active in SCV-infected fatal Rhesus monkey kidney (FRhK-4) cells[24], distinct from other active siRNA reported by other labs[25–28]. However, translation of *in vitro* siRNA activity into clinically useful therapeutics depends on a clinically acceptable means for administration. Therefore, siRNAs showing prominent prophylactic and therapeutic activity in cell culture[24], referred to as siSC2 and siSC5, were further evaluated *in vivo*, first using a reporter gene assay in mice and subsequently using a clinically acceptable intranasal administration in the recently established Rhesus macaque SARS model[21,22]. The study provided strong evidence that these siRNA agents are potent both for prophylactic and therapeutic treatment of SARS infection, and they lack toxicity in this nonhuman primate model. The results support the growing expectation that siRNA can fulfill the need for moving rapidly from gene sequence to targeted therapeutic agents for many previously intractable disease targets.

[1]Biotechnology Research Center of Sun Yatsen University, and Key Laboratory of Gene Engineering of Ministry of Education of the State, Guangzhou, China. [2]Guangzhou Top Genomics, Ltd., Guangzhou, China. [3]Intradigm Corporation, 12115 K Parklawn Drive, Rockville, Maryland 20852, USA. [4]Institute of Laboratory Animal Science, Chinese Academy of Medical Sciences & Peking Union Medical College, Beijing, China. [5]Department of Pathology, University of Hong Kong, Hong Kong, China. [6]Guangzhou Institute of Respiratory Diseases, Guangzhou, China. [7]These authors contributed equally to this work. Correspondence should be addressed to P.Y.L. (patricklu@intradigm.com) or N.Z. (nanshan@vip.163.com).

Published online 21 August 2005; doi:10.1038/nm1280

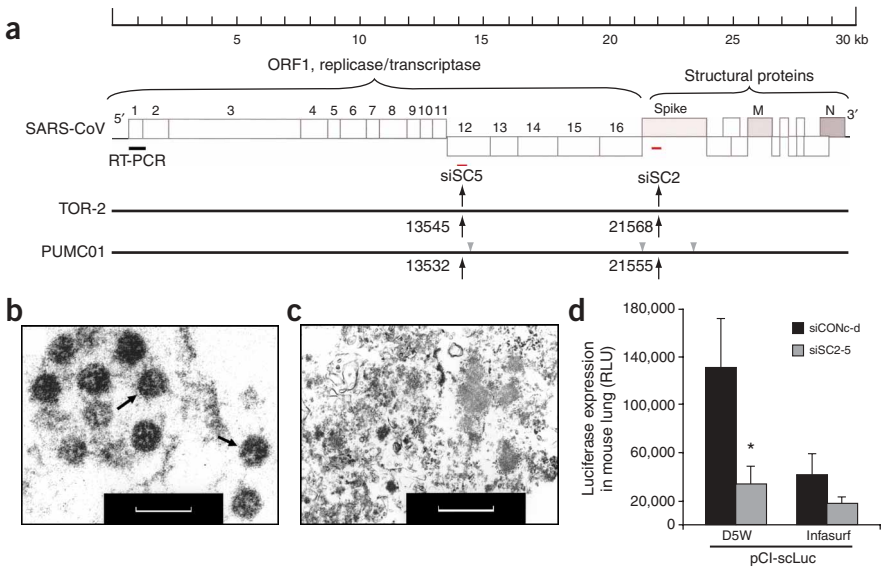

Figure 1 Selection and validation of siRNA duplexes targeting SCV sequence. (**a**) The RT-PCR–amplified region is marked at the most upstream region of open reading frame 1 (ORF1). The siSC2- and siSC5-targeted regions (red dashes) were also marked within the Spike- and NSP12-coding regions of the SCV genome, respectively. Black arrows indicate the locations of the two targeted sequences within the viral RNA genome and gray arrowheads indicate mutation sites. Electron microscopy images of SCV particles are indicated by arrows within SCV-infected FRhK-4 cell (**b**) and the SCV-infected FRhK-4 cell treated with siSC2-5 (**c**). Scale bar in **b** and **c**, 200 nm. (**d**) Luciferase expression (measured in relative luciferase units, RLU) in mouse lungs after co-delivery of the expression plasmid pCI-scLuc and either siSC2-5 or siCONc-d, in either D5W or Infasurf solution. $^*P < 0.05$, $n = 5$.

RESULTS

Selection of potent anti-SCV siRNAs

Two siRNA duplexes, siSC2 and siSC5, targeting the SCV genome at Spike protein–coding and ORF1b (NSP12) regions (**Fig. 1a**), respectively, were chosen for *in vivo* studies for the following reasons: (i) their targeted sequences show a 100% homology to strain TOR-2 used in the cell-culture study[24], to strain PUMC01 used in the macaque model[21,22] and to another 100 published SCV strains isolated during different phases of SCV evolution as recently defined[6] with wide geographic distributions around the world; (ii) they are the two most potent inhibitors for reducing SCV replication in FRhK-4 cells among a set of active siRNA duplexes selected from 48 siRNA duplexes targeting the entire SCV genome[23,24]; (iii) a synergistic anti-SCV activity was observed when a combination of siSC2 and siSC5 was applied in the cell-culture study showing the strongest prophylactic and therapeutic effects (**Fig. 1b**,**c**)[24]; (iv) their targeted sequences share no homology with the human genome, avoiding potential nonspecific knockdown of the endogenous genes of an individual receiving this type of treatment. In addition, two unrelated siRNA duplexes, siCONa and siCONb, with no homology to either the human genome or the SARS genome, validated in the cell-culture study[24], show no RNAi activity for SCV inhibition, and were chosen as the negative control (**Supplementary Fig. 1** online).

siSC2 and siSC5 duplexes were active in mouse lung

To insure *in vivo* activity of the siSC2-siSC5 combination (siSC2-5) with a clinically viable delivery method we first established a luciferase-based reporter gene system, containing both siSC2 and siSC5 targeted sequences between a cytomegalovirus promoter and the luciferase coding region. Cotransfection of pCI-scLuc and siSC2-5 into cultured cells confirmed that siSC2-5 can specifically knock down luciferase expression (data not shown). To identify a clinically viable carrier for siRNA delivery into mouse lung, we selected two carriers currently in clinical use, D5W solution[29] and Infasurf solution[30], which have been applied in delivery of DNA[31] and siRNA[32] to animal models. Twenty-four hours after intratracheal administration of 30 μg of pCI-scLuc plasmid DNA and 30 μg of siSC2-5 in 100 μl of D5W or Infasurf solution into BALB/c mouse lungs, we analyzed luciferase expression in the lung tissues. Co-delivery of pCI-scLuc plasmid with siSC2-5 in D5W solution resulted in a higher level of reporter gene expression and a stronger RNAi effect than that delivered in the Infasurf solution (**Fig. 1d**). We noted that TransIT-TKO and polyethyleneimine have been reported as carriers for intranasal[33], intratracheal[34] and intravenous[35] deliveries of siRNA into mouse models for treatment of influenza virus and respiratory syncytial virus infections. But those carriers are not feasible for clinical use, especially polyethyleneimine, because it can induce severe lung inflammation through either intravenous or intratracheal delivery in mice based on our experience (data not shown) and literature reports[36,37]. The substantial silencing effect achieved in mouse lungs strongly supported that siSC2-5 is a potent inhibitor of SCV RNA, but also that D5W is a very effective carrier for siRNA in the mammalian respiratory tract. In addition, a lack of visible lung damage after intratracheal delivery of 30 μg siRNA and 30 μg plasmid DNA together provided a safe baseline for siRNA dosing to the respiratory tract of larger mammals.

SCV-induced SARS-like symptoms in monkey

We used a total of 21 macaques in this study, including five groups ($n = 4$) infected with SCV and one individual without SCV infection. The five groups consisted of two control groups—viral infection control and nonspecific siRNA control—and three treatment regimen groups—prophylactic treatment, co-delivery treatment and postexposure treatment. After anesthetizing the macaques, we infected them with SCV at a dosage of 105 times the half-maximal tissue culture infectious dose ($TCID_{50}$) in 1 ml PBS solution through intranasal instillation. We also administered the siSC2-5 or the combination of siCONa and siCONb (siCONa-b) through the same route at 30 mg per dose in 3 ml D5W solution, with different dosing regimens (**Table 1**).

Initial observations indicated that all SCV-infected macaques developed SARS-like symptoms, but those in the control groups showed a greater severity than that reported in the cynomolgus macaque SARS model[19]. For example, all macaques in the viral infection control group and the nonspecific siRNA control group developed an elevated body temperature, in some cases lasting for the entire 20-d study period. In contrast, 10 of 12 macaques from the siSC2-5–treated groups showed a milder elevation of body temperature. All animals displayed a loss of appetite and some became agitated and aggressive. General observation of the lung histology specimens indicated that lung lesions developed with congestions and palpable

Table 1 Study design and dosing regimen

Groups	Viral infection control	Nonspecific sequence control	Prophylactic treatment	Co-delivery treatment	Postexposure treatment
Cohort ($n = 4$)	007, 205, 206, 212	163, 167, 202, 208	130, 138, 151, 203	002, 021, 077, 166	210, 015, 214, 023
Sex	M, M, F, F	M, M, F, F	F, F, M, M	F, M, M, F	F, M, M, F
Age (years)	3	3	3	3	3
Body weight	3.4 ± 0.2	3.6 ± 0.2	3.4 ± 0.2	3.7 ± 0.3	3.1 ± 0.5
Viral dosage (1 ml)	10^5 $TCID_{50}$	10^5 $TCID_{50}$	10^5 $TCID_{50}$	10^5 $TCID_{50}$	10^5 $TCID_{50}$
siSC2-5			30 mg/3 ml/dose	30 mg/3 ml/dose	30 mg/3 ml/dose
siCONa-b		30 mg/3 ml/dose			
Dosing regimen	–4 h		√		
	Co-delivery	√		√	
	4 h				√
	24 h	√		√	√
	72 h	√		√	√
	120 h	√		√	
Total dosage		120 mg/120 h	30 mg/120 h	120 mg/120 h	90 mg/120 h
Termination at Day 7:	205, 206	167, 202	138, 151	002, 077, 166	015, 210
Termination at Day 20:	007, 212	163, 208	130, 203	021	023, 214

We used 20 Rhesus monkeys belonging to five test groups in the study with the same viral titer challenge but different drug dosing regimens of siRNA. We tested four monkeys in each group and necropsied at either 7 or 20 d.p.i. in a biohazard level 3 environment. We used one additional monkey, #921, as a 'no viral infection' control and collected lung tissue for histology analysis. Cohort indicates groups of monkeys and numbers indicate macaque identification numbers. Termination indicates that observations were terminated because animals were killed.

nodules, which were scattered in distribution and were localized particularly at the posterior part of different lobes[22]. The most severe lung damage occurred focally and was surrounded by large areas of obvious pathology, whereas milder lung damage appeared with smaller areas of pathology.

To better characterize the pathological changes, we adopted a six-grade scoring system to describe the severity of the lung damage from least severe to most severe: (i) "–", (ii) "±", (iii) "+", (iv) "++", (v) "+++" and (vi) "++++" (**Fig. 2a–f**). Liver enzymatic analysis showed an evident increase of alanine aminotransferase, lactic acid dehydrogenase, creatine kinase and aspartate aminotransferase after SCV infection of all 20 macaques from every tested group, at 7 d.p.i. Notably, routine blood examination indicated a marked increase of hemoglobin and platelets in all SCV-infected macaques, which is contradictory to other reports on the SARS macaque model[20] and on SARS-infected individuals[9,10,15] (**Supplementary Tables 1** and **2** online). The mechanism underlying the differences in behavior of these primate SARS models requires further investigation.

SCV infection caused acute DAD in monkey lungs

SCV-induced DAD in the lower airway usually is observed in individuals with SARS who have had the disease for more than 10 d[9], whereas the SCV-infected macaque lungs started developing acute DAD at 4 d.p.i.[19,22]. In histopathological and immunohistochemical (IHC) inspections, we found that most of the lungs, at both 7 and 20 d.p.i., displayed acute DAD with various degrees of severity. The typical features of SCV infection–induced lung damage include broken alveolar walls and interstitial edema (**Fig. 3a**), hyaline membrane formation along the alveoli and pneumocyte desquamation (**Fig. 3b**), damaged alveolus filled with hemorrhage and pneumocytes with nuclear enlargement, prominent nucleolus and amphophilic granular cytoplasm (**Fig. 3c**), and interstitial infiltrates with neutrophils, lymphocytes and macrophages (**Fig. 3d**). Within damaged lung tissues, we identified viral-infected pneumocytes, infiltrated neutrophils, lymphocytes and monocytes using IHC stains of keratin (**Fig. 3e**), CD68 (**Fig. 3f**), CD4, CD8 and CD35 (data not shown). These characteristics were very similar to those observed in individuals with SARS[9,10] and SARS macaque models[19–22]. Therefore, this Rhesus macaque model provides an ideal system for evaluation of new therapeutic agents against SARS.

siRNA suppressed SARS-like symptoms

The body temperature of the infected macaque is a key indicator not only for the severity of SARS-like symptoms but also for effectiveness of the treatment. We recorded body temperature of every animal daily until it was killed. Comparison of the mean body temperatures of all

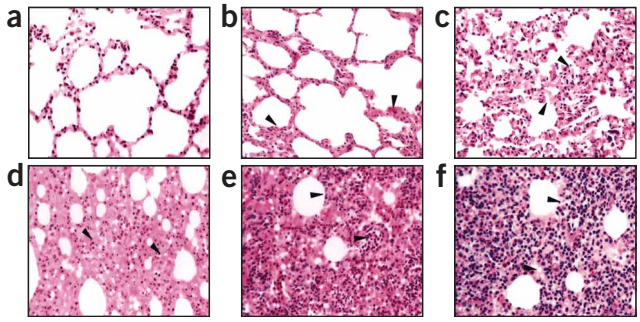

Figure 2 Severity of lung histopathology in SCV-challenged macaques. All lung histology sections were stained with H&E (original magnification, ×100). (**a**) Normal lung section from macaque #921 without SCV infection "–". (**b**) Minor inflammation "±", from macaque #138, slight broadening of alveolar septa and sparse monocyte infiltration. (**c**) Apparent inflammation "+", from macaque #077, hemorrhage in septa, elastic fibers of alveolar wall distorted as shown by silver staining. (**d**) Early symptom of acute DAD "++", from macaque # 015, alveolus septa broadening with increasing infiltration of inflammatory cells. (**e**) Typical symptom of acute DAD "+++", from macaque #212, extensive exudation and septa broadening, shrinking of alveoli caused by pressure, restricted fusion of the thick septa, obvious septa hemorrhage, ruptured elastic fiber of alveolar wall and slight cell infiltration in alveolar cavities. (**f**) Severe acute DAD "++++", from macaque #202, massive cell filtration and alveoli shrinking, sheets of septa fusion, necrotic lesions at the hemorrhagic septa and massive cell infiltration in alveolar cavities.

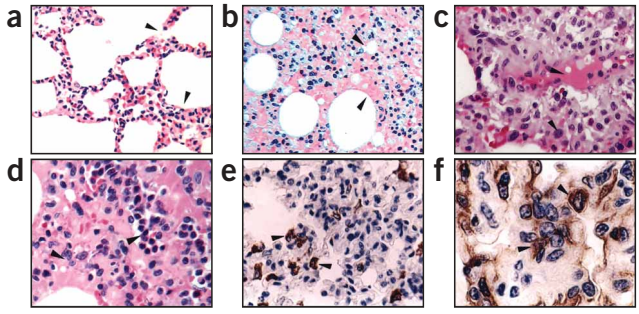

Figure 3 Histopathological characteristics of SCV-infected macaque lungs. (**a**,**b**) Lung sections were stained with H&E (original magnification, ×100). (**a**) Section from macaque #214 shows the alveolar walls collapsed and acute diffuse interstitial injury with interstitial edema (arrows) at an early stage of the disease. (**b**) Section from macaque #015 shows hyaline membrane formation (arrows) along the alveoli and pneumocyte desquamation. (**c**,**d**) Lung sections stained with H&E (original magnification, ×200). (**c**) Section from macaque #166 shows that damaged alveoli were filled with hemorrhage and inflammatory cells (upper arrows) and pneumocytes with nuclear enlargement, prominent nucleolus and amphophilic granular cytoplasm resulting in focal giant-cell formation (lower arrows). (**d**) Section from macaque #202 shows inflammatory cells, including neutrophils, lymphocytes, macrophages and monocytes, were present in the damaged alveoli. (**e**) IHC staining of SCV-infected monkey lung section with keratin-specific monoclonal antibody indicates the epithelial origin of the pneumocytes (arrows) (original magnification, ×200). (**f**) IHC staining of SCV-infected monkey lung section with CD68 monoclonal antibody indicates microphage infiltrates (arrows) (original magnification, ×500).

five groups (**Fig. 4a**) revealed significantly lower temperatures of all treated groups (prophylactic, co-delivery and postexposure treatment groups; below 38.9 °C) versus the control groups (viral infection and nonspecific siRNA groups), which had temperatures above 39.1 °C, indicating a fever status[22]. The prophylactic treatment group had the lowest temperature (38.7 °C), close to the normal body temperature of Rhesus monkey (38.5 °C). Examining the distribution of the average body temperature at each time point throughout the entire 20-d period with trend regression (**Fig. 4b**), we found that viral infection and nonspecific siRNA control groups had consistently elevated temperatures above 39 °C. Macaque #212 from the viral infection control group had a high fever (40 °C) at 4 d.p.i. and the fever lasted until the macaque was killed at 20 d.p.i. for pathology analysis, at which time it showed a severe lung damage that we scored as "+++". A similar situation was seen for macaque #208 of the nonspecific siRNA group. The comparison of mean body temperature trend regression clearly shows the prophylactic and therapeutic effects of siSC2-5 on suppression of fever induced by SCV infection. In addition, the inhibitory effects of siSC2-5 also resulted in lowering SCV-specific IgG titer in blood samples (**Fig. 4c**). We detected SCV-specific IgG levels in viral control and nonspecific siRNA control groups as early as 10 d.p.i., but not in the co-delivery and post-exposure treatment groups. We were able to detect SCV-specific IgG titers of all groups at 19 d.p.i.

siRNA protected lung from severe acute DAD

In the viral infection control group, macaques #212 and #206 had severe acute DAD with pathological changes in a large portion of the lungs, including interstitial infiltrates and lung damage that we scored as "+++". Macaque #202 of the nonspecific siRNA control group showed even more severe acute DAD in a large portion of the lung, with massive cell infiltration and alveoli shrinkage, sheets of septa fusion, necrotic lesions at the hemorrhagic septa and extensive loss of alveolar and bronchiolar epithelium, representing a typical lung damage score of "++++", the worst case among all 20 SCV-exposed macaques. All macaques from both viral infection and nonspecific siRNA control groups suffered from severe acute DAD with a lung damage score of "+++". On the other hand, lung tissues from all three siSC2-5–treated groups (prophylactic, co-delivery and postexposure treatment groups) showed relatively mild severity of acute DAD and none showed lung damage beyond a score of "++". The comparison of lung histopathlogical scores of all groups

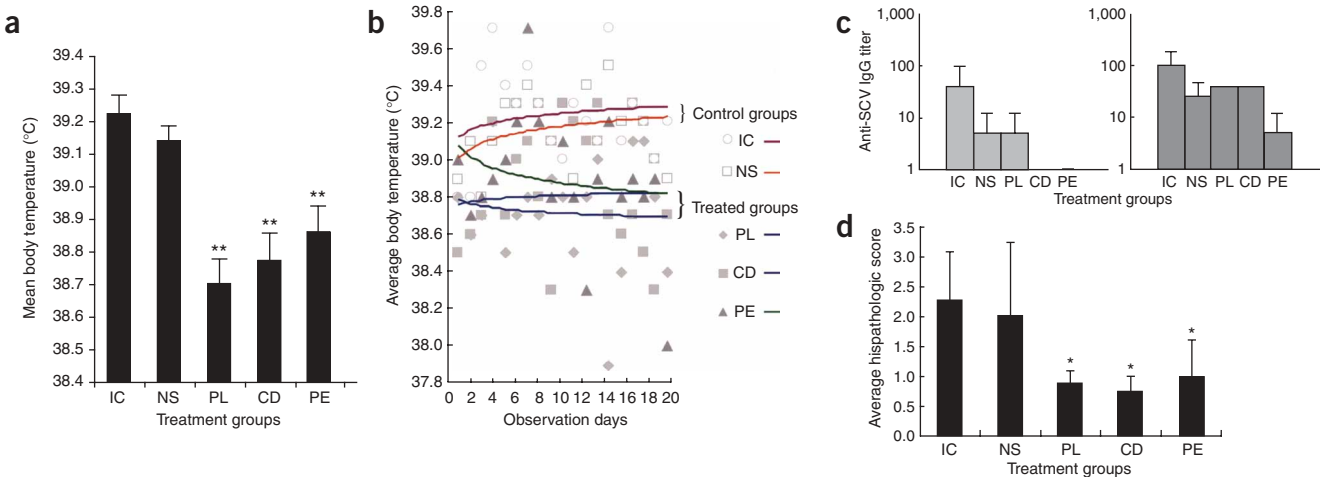

Figure 4 siSC2-5 relieved SARS symptoms. (**a**) Comparison of mean body temperature. Mean body temperature represents mean value of average body temperature of each group during the 20-d period. $^{**}P < 0.01$ for *t*-test compared to viral infection control group, $n = 20$. IC, viral infection control; NS, nonspecific siRNA control; PL, prophylactic treatment; CD, co-delivery treatment; PE, postexposure treatment. (**b**) Distribution of the average body temperatures throughout the 20-d period. The regression analysis was conducted based on the average body temperature of each group on each day. The average body temperature of each group was calculated with $n = 4$ before 7 d.p.i. and $n = 2$ afterward. (**c**) IgG titers of SCV-specific antibody in serum samples were measured at 10 d.p.i. (left) and 19 d.p.i. (right). (**d**) The average histopathological scores of each group, including lung samples collected at both 7 d.p.i and 20 d.p.i, were compared against the viral infection control group. $^{*}P < 0.05$, $n = 4$.

indicates that the siSC2-5–treated macaques were protected from severe acute DAD (**Fig. 4d**).

siRNAs inhibited SCV replication in monkey respiratory tract

We analyzed oropharyngeal swab samples at 4 d.p.i. with quantitative real-time PCR (Q-RT-PCR). They showed that SCV viral RNA was detectable in all samples from the viral infection and nonspecific siRNA control groups, but undetectable in 75% of the samples from the siSC2-5 treatment groups (**Fig. 5a**). This result indicated the possible inhibition of SCV infection and replication through siSC2-5–facilitated viral RNA degradation in upper airway epithelial cells. The three positive samples from the treatment groups suggest that the dosing regimens were unable to totally eliminate SCV infection. The histopathology analyses of those macaques (#130, 166 and 210) have indeed shown some degrees of lung damage at scores of "+" or "++". The Q-RT-PCR detection of the randomly selected lung tissue specimens also showed the presence of the SCV RNA (**Supplementary Fig. 2** online). We also applied the oropharyngeal swab samples for active viral rescue in the Vero cell culture, showing that samples from all five groups were positive for live SCV particles. To evaluate SCV infection in deeper lung, we carefully inspected IHC staining images from each lung section, with SCV antigen–specific monoclonal antibody. The samples from viral infection and nonspecific siRNA groups presented much more infected cells (**Fig. 5b–d**) than those from siSC2-5–treated groups (**Fig. 5e–g**). The SCV-infected cells include the type I pneumocytes (**Fig. 5c**,**e**), type II pneumocytes (**Fig. 5f**) and macrophages (**Fig. 5d**), the presence of which was consistent with the observation in the previous studies with macaque models and in individuals with SARS[4,9,10,19–22]. We further counted the infected cells in each lung section and compared these numbers for the five groups. The lungs from all three siSC2-5 treatment groups had significantly lower counts of the SCV-infected cells (**Fig. 5h**), which indicated that the siRNA treatments were able to inhibit SCV replication and spread within the monkey lungs.

siRNA was safe for prophylactic and therapeutic treatments

Evaluation of a new biological agent such as siRNA for its therapeutic utility depends not only on its efficacy in treating diseases, but also on its tolerability and safety. Our study put both efficacy and safety in equal consideration in order to define a therapeutic window for use of siRNA as an anti-SARS agent through airway administration. The choice of the siSC2-5 dosage at 10 mg/kg was based on the mouse study described above and study reports on antisense oligomers[38]. Through observation of behavior patterns of Rhesus macaques during the entire study and examination of the organs of killed animals with various siRNA dosing regimens, no safety concerns arose. The treatment groups lacked evidence of inflammation or toxicity not attributable to the SCV infection. The total accumulated dosage of siRNA administrated to individual macaques ranged from 10 mg/kg to 40 mg/kg and did not cause any visible differences in appearance, behavior or sign of organ damage when examined by autopsy and necropsy. In addition, we found no statistically significant differences in internal organ coefficients among the five groups (**Supplementary Table 3** online). Reports of potential 'off-target' effects of the siRNA agent[39–41] have been mostly based on cell-culture experiments, without evidence for *in vivo* siRNA toxicity[29,31]. From the results of routine blood examination and liver enzymatic analysis, we found some increases of alanine aminotransferase, lactic acid dehdryogenase, creatine kinase, aspartate dehydrogenase, hemoglobin and platelet levels in the blood samples. Because those increases are from SCV-infected macaques, with or without siRNA treatment, they were probably results from the viral infection rather than the siRNA treatments (**Supplementary Tables 1** and **2** online).

DISCUSSION

Although concern remains over whether the macaque SARS models are clinically relevant[14,20–22], the Rhesus macaque model used here, which used the high-virulence SCV strain PUMC01 (ref. 6), mirrors the sequence of pathogenesis in humans with SARS[9,10]

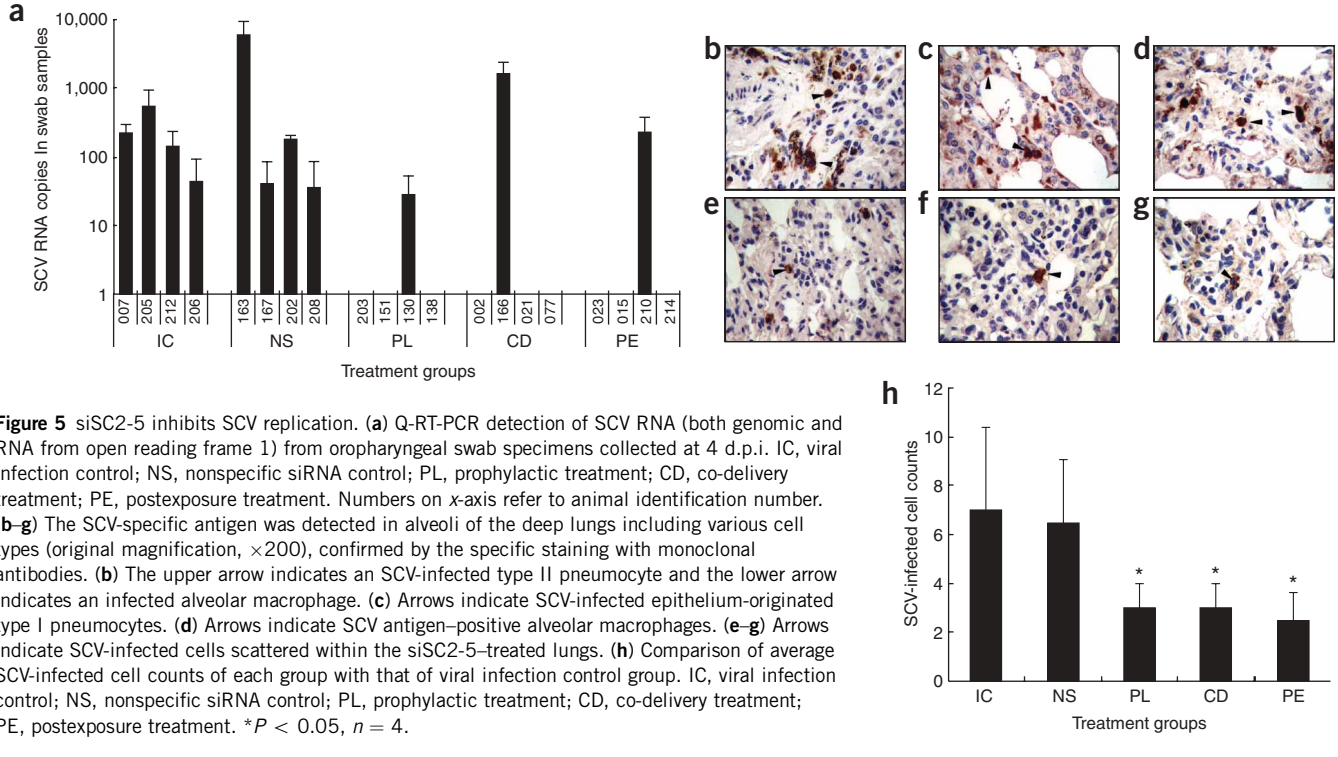

Figure 5 siSC2-5 inhibits SCV replication. (**a**) Q-RT-PCR detection of SCV RNA (both genomic and RNA from open reading frame 1) from oropharyngeal swab specimens collected at 4 d.p.i. IC, viral infection control; NS, nonspecific siRNA control; PL, prophylactic treatment; CD, co-delivery treatment; PE, postexposure treatment. Numbers on *x*-axis refer to animal identification number. (**b**–**g**) The SCV-specific antigen was detected in alveoli of the deep lungs including various cell types (original magnification, ×200), confirmed by the specific staining with monoclonal antibodies. (**b**) The upper arrow indicates an SCV-infected type II pneumocyte and the lower arrow indicates an infected alveolar macrophage. (**c**) Arrows indicate SCV-infected epithelium-originated type I pneumocytes. (**d**) Arrows indicate SCV antigen–positive alveolar macrophages. (**e**–**g**) Arrows indicate SCV-infected cells scattered within the siSC2-5–treated lungs. (**h**) Comparison of average SCV-infected cell counts of each group with that of viral infection control group. IC, viral infection control; NS, nonspecific siRNA control; PL, prophylactic treatment; CD, co-delivery treatment; PE, postexposure treatment. $^*P < 0.05$, $n = 4$.

and the cynomolgus macaque SARS model[1,19]. Clear clinical relevance of this model can be found in most of the parameters studied, including elevated body temperature, lung pathology and SCV antigen detection in epithelial-originated type I pneumocytes, type II pneumocytes and macrophages, providing strong support that the model has the attributes required for evaluation of siRNA candidate therapeutic agents.

Here we administered siSC2-5 by the same intranasal route as the SCV challenge, with prophylactic, concurrent or early postexposure treatments within a period of 5 d.p.i. All three different treatment regimens achieved potent suppression of SCV-induced SARS pathogenesis. Detection of SCV RNA genome with RT-PCR showed that only 25% of oropharyngeal swab samples from the treated group were positive versus all samples from the control groups. Similarly, using IHC detection, SCV-infected cell counts were significantly decreased in the lung sections from the treated groups. Along with the reduced viral load was a substantial reduction in SARS-like symptoms and lung histopathology, including significantly lowered mean body temperatures in all siSC2-5–treated groups, and no lung damage beyond a score of "++". In contrast, the mean body temperatures in the control groups indicated a fever status, along with substantial lung damage of "+++" or "++++".

We designed this study to investigate siRNA-mediated anti-SCV effects in both the upper airway and deep lung of SCV-exposed macaques that occurred during an early phase of viral infection and disease progression. The impact of siSC2-5 on the early phase of SCV infection was first shown in the mucosal epithelial cells of the upper respiratory tract, as expected because both the siSC2-5 and SCV were administered through intranasal instillation and all siRNA dosing was complete within the first 5 d. This anti-SARS efficacy of siSC2-5 could be the result of one or more of the following three mechanisms: protection of cells from SCV infection, degradation of SCV mRNA inhibiting viral protein synthesis in infected cells[24], or obstruction of SCV genome replication and spread to uninfected cells. Considering that SARS-specific neutralizing antibody in SCV-infected macaques can be detected as early as 10 d.p.i., we speculated that the clinical benefit of siRNA-mediated anti-SARS activity observed in this study was the consequence of combined activities of the siRNA agent and the neutralizing antibody, suggesting that multiple antiviral mechanisms were operative.

Delivering siSC2-5 before SCV infection in the prophylactic treatment group using a single dose was able to achieve a comparable inhibitory effect to that of the co-delivery and postexposure treatment groups. The prophylactic anti-SCV activity resulted in a lower body temperature, milder lung damage, less viral RNA detected and lower numbers of SCV-infected cells in the lung, in comparison with co-delivery and postexposure treatment groups. The mechanism of action might be the result of direct degradation of viral RNA by preexisting siSC2-5 within the upper airway cells upon entry of the viral particle, blocking replication and spread of SCV particles. In addition, a cellular antiviral activity induced by siRNA transfection other than an interferon response may also have a role[24].

The interferon response to siRNA duplexes as in cell-culture studies has raised concerns about the specificity of RNAi in animals[42–45]. But a recent *in vivo* study using siRNA against RSV in mouse lung showed a lack of detectable siRNA-induced interferon[29]. This observation was also echoed by a report that intravenous siRNA delivery in mice resulted in a lack of interferon induction *in vivo*[46]. The siSC2-5 and siCONa-b we used in the study contain neither the 5′-UGUGU-3′ nor the 5′-GUCCUUCAA-3′ motifs suspected to be immunostimulatory elements when in association with transfection reagents[44,45]. We did not find anti-SCV activity when using the control siCONa-b. Therefore, we conclude the anti-SARS activity is probably the result of siSC2-5–mediated SCV RNA degradation within cells throughout the pulmonary tracts of the treated macaques.

Release of proinflammatory cytokines from alveolar macrophages has been proposed to have a prominent role in SARS pathogenesis and to be a point for intervention[9]. The presence of hemophagocytosis[47,48] or an interferon-γ–related cytokine storm in individuals with SARS[49] complicates our understanding of SARS pathogenesis but also argues against use of interferon therapy in clinical treatment, despite studies in cell culture[18], a macaque model[19] and individuals with SARS[50] that showed inhibition of SCV with interferon treatment. In contrast to such proinflammatory cytokine treatments, intranasal delivery of siRNA offers a unique method for high-specificity inhibition of SCV with minimal induction of a proinflammatory cytokine antiviral response that may help to avoid exacerbation of symptoms and lung damage. Here, we present evidence for a strong anti-SARS activity without any visible adverse effects through intranasal administration of siSC2-5 in a clinically viable aqueous solution with a nonhuman primate SARS model. Our data suggest that clinical testing of siSC2-5 agent as a SARS treatment is warranted. This work also shows the tremendous potential for siRNA to enable rapid development of treatments for emerging infectious agents, and for powerful 'targeted' therapeutics acting at the level of gene expression.

METHODS

SCV and Rhesus macaque model. The SCV strain PUMC-01 was isolated from an individual in the Peking Union Medical Hospital and propagated in cultured Vero cells. The Rhesus macaque (*Macaca mulatta*) SARS model was developed using intranasal inoculation of PUMC01 SCV[21,22]. We performed our studies in Biosafety Level 3 laboratories exclusively assigned for SCV research at the Institute of Laboratory Animal Science of Chinese Academy of Medical Sciences, after approval of our animal study protocol by the Institutional Animal Welfare Committee. We inoculated monkeys with PUMC01 (10^5 TCID50/1.0 ml) through intranasal instillation, mimicking the natural route of SCV infection of humans with SARS. We also delivered 30 μg of siSC2-5 and siCONa-b in 3 ml of D5W solution with intranasal instillation. We confirmed that all monkeys were negative for the presence of SCV-specific antibody before SCV challenge.

After the SCV challenge and siRNA dosing, we observed the clinical signs of the macaques daily, including body temperature, size of lymph nodes, body weight, coughing, sneezing, appetite, aggressiveness, etc. At 4 d.p.i., we took oropharyngeal swabs from SCV-challenged monkeys for detection of viral RNA using RT-PCR and viral re-isolation. We collected blood samples on 4, 7, 10 and 19 d.p.i. for routine laboratory examination, including liver enzymatic analysis and the detection of SCV-specific antibody. The ELISA Diagnosis kits for detection of SCV-specific IgG or IgM (Hau Da Biotech) were used according to the manufacturer's protocol.

We collected lungs after necropsy of the macaques at 7 and 20 d.p.i. for histopathological analyses. We also collected other organs for inspection of morphology and appearance, followed by comparison of the internal organ coefficients of each group, based on wet weight of organ per 100 g of average body weight (**Supplementary Table 3** online).

siRNA duplexes. We selected two SCV-specific siRNA duplexes, siSC2 and siSC5, based on a previous *in vitro* study[24] and used them as a mixture (siSC2-5) consisting of an equal amount of each siRNA duplex. We also used a pair of control siRNA duplexes, siCONa and siCONb, as a mixture (siCONa-b). We used another pair of unrelated control siRNA duplexes, siCONc and siCONd, as a mixture in the mouse study (siCONc-d). All siRNA duplexes consisted of two complementary 21-nucleotide RNA strand with 3′ dTdT overhangs, and were chemically synthesized (Qiagen). siRNA sequences were as follows: siSC2: (forward) 5′-GCUCCUAAUUACACUCAACdtdt-3′, (reverse) 3′-dtdtCGAGGAUUAAUGUGAGUUG-5′; siSC5: (forward) 5′-GGAUGAGG AAGGCAAUUUA dtdt-3′, (reverse) 3′-dtdtCCUACUCCUUCCGUUAAAU-5′;

siCONa: (forward) 5′-CCGCUGGAGAGCAACUGCAdtdt-3′, (reverse) 3′-dtdt GGCGUCCUCUCGUUGACGU-5′; siCONb: (forward) 5′-GCUAUGAAACGA UAUGGGCdtdt-3′, (reverse) 3′-dtdtCGAUACUUUGCUAUACCCG-5; siCONc: (forward) 5′-GCUGACCCUGAAGUUCAUCdtdt-3′, (reverse) 3′-dtdtCGACU GGGACUUCAAGUAG-5′; siCONd: (forward) 5′-GCAGCACGACUUCUU CAAGdtdt-3′, (reverse) 3′-dtdtCGUCGUGCUGAAGAAGUUC-5′.

Electron microscopy. We harvested FRhk-4 cells infected by SCV, with or without siSC2-5 treatment, and fixed them in epoxy resin (Polysciences). We examined ultrathin sections (70 nm thick) under a Philips EM208S electron microscope at 80 kV as described previously[24].

Delivery of nucleic acid into mouse lungs. We divided 20 6–8-week-old BALB/c mice into four groups ($n = 5$). We tested two carrier solutions, RNase-free D5W (5% D-glucose in water, wt/vol, made in-house) and Infasurf solution (ONY Inc.), for delivering siSC2-5, siCONc-d and pCI-scLuc plasmid. We mixed 30 μg of pCI-scLuc and 30 μg of corresponding siRNAs in 100 μl carrier solutions and intratracheally administered them into the mouse lungs. We constructed the pCI-scLuc plasmid by inserting a DNA fragment containing siSC2- and siSC5-targeted sequence DNA between its cytomegalovirus promoter-driven transcriptional initiation site and luciferase-coding sequence. At 24 h after delivery, mice were killed and lung tissues were harvested and homogenized in 800 μl of 1× Reporter Lysis buffer (Promega) using Lysing Matrix D (Bio 101 System) in a FastPrep-FP120 (Bio 101 System) at speed 4.0 for 40 s. After centrifugation at 12,000 r.p.m. for 2 min at 4 °C, we used 10 μl of supernatant for measurement of luciferase activity using a Luciferase Assay kit (Promega) and a luminometer (Analytical Luminescence Laboratory) following the manufacturer's protocol. We performed the animal experiment under a protocol approved by the Institutional Animal Care and Use Committee of the Biomedical Research Institute.

Q-RT-PCR and SCV re-isolation. We isolated total cellular RNA using a QIAamp RNA isolation kit (Qiagen). We synthesized the first strand cDNA using RNAse H^+ reverse transcriptase and random primers (Invitrogen), according to the manufacturer's protocol. The forward and reverse primers, targeting upstream of open reading frame 1 (ORF1), and the fluorescent probe used for PCR are: 5′-GCATGAAATTGCCTGGTTCAC-3′ (ORF1 forward), 5′-GCATTCC CCTTTGAAAGTGTC-3′ (ORF1 reverse) and FAMAGCTACGAG CACCAGACACCCTTCGAAATRMA (fluorescent probe for PCR). We performed RT-PCR using ABI7900 Sequence Detection System (ABI). All PCR experiments were done in triplicate[24]. We conducted SCV re-isolation using the swab samples by serial passage on Vero cell culture as previously described[21,22].

Lung histopathology and IHC analyses. We obtained lung tissue blocks from the right upper and right middle lobes and performed pathology analysis as described previously[22]. We determined the severity of lung damage based on observations of five different sections of each lung by readouts from three independent pathologists who were blinded to experimental conditions. To quantify pathological changes in lung after the treatment, we calculated the average histopathlogical scores of each group using the scoring system described above. We de-waxed wax-embedded tissue sections and rehydrated them for the IHC analysis as described previously[22]. We identified the cell types based on the separate staining with corresponding monoclonal antibodies using methods described previously[21,22]. We used viral antigen detection with IHC to indicate infected cells. We collected the SCV-infected cell counts within each microscopic image from every lung tissue section independently by three readouts with investigators blinded to the experimental conditions. We compared average cell counts of four lungs from each group ($n = 4$).

Statistical analysis. We analyzed data using the Student *t*-test for luciferase expression in mouse lungs, mean body temperature, histopathology score comparison and SCV-infected cell counts. We considered results statistically significant only when $P < 0.05$. We conducted the regression analysis based on the average body temperature of each group at each day point. We conducted the multifactor ANOVA for the internal organ coefficient.

Accession codes. GenBank: SCV strain PUMC01, AY350750; strain TOR-2, AY274119; SCV complete genome sequence, NC-004718.

Note: Supplementary information is available on the Nature Medicine website.

ACKNOWLEDGMENTS

This study was supported in part by the Science and Technology Commission, Guangdong Provincial Government, Guangzhou Science and Technology Bureau, Guangzhou Economic & Technological Development District, and China World Trade Corporation (Guangzhou), Top Biotech, Ltd. (Hong Kong), China. We thank C. Lu, X.S. Zhang and D.C. Zheng of Top Genomics, Ltd. (Guangzhou) for their administrative work to coordinate and facilitate the study; H. Gao, X.M. Tu, L.L. Bao, W. Deng and B.L. Zhang of Institute of Laboratory Animal Science and L. Ruan of Institute of Virology, Chinese Academy of Medical Sciences & Peking Union Medical College, Beijing, for their supports during the study; W. Tian and E. Lader of Qiagen for their collaborative efforts; Y.Y. Gu of Guangzhou Institute of Respiratory Diseases for her advice on lung pathological analysis; and ONY Inc. Amherst, New York, USA for providing Infasurf.

COMPETING INTERESTS STATEMENT

The authors declare competing financial interests (see the *Nature Medicine* website for details).

Received 18 November 2004; accepted 10 July 2005
Published online at http://www.nature.com/naturemedicine/

1. Fouchier, R.A. *et al.* Aetiology: Koch's postulates fulfilled for SARS virus. *Nature* **423**, 240 (2003).
2. Kuiken, T. *et al.* Newly discovered coronavirus as the primary cause of severe acute respiratory syndrome. *Lancet* **362**, 263–270 (2003).
3. Ksiazek, T.G. *et al.* A novel coronavirus associated with severe acute respiratory syndrome. *N. Engl. J. Med.* **348**, 1953–1966 (2003).
4. Peiris, J.S. *et al.* Coronavirus as a possible cause of severe acute respiratory syndrome. *Lancet* **361**, 1319–1325 (2003).
5. Guan, Y. *et al.* Isolation and characterization of viruses related to the SARS coronavirus from animals in southern China. *Science* **302**, 276–278 (2003).
6. Chinese SARS Molecular Epidemiology Consortium. Molecular evolution of the SARS coronavirus during the course of the SARS epidemic in China. *Science* **303**, 1666–1669 (2004).
7. Snijder, E.J. *et al.* Unique and conserved features of genome and proteome of SARS-conronavirus, an early split-off from the coronavirus group 2 lineage. *J. Mol. Biol.* **331**, 991–1004 (2003).
8. Marra, M.A. *et al.* The genome sequence of the SARS-associated coronavirus. *Science* **300**, 1399–1404 (2003).
9. Nicholls, J.M. *et al.* Lung pathology of fatal severe acute respiratory syndrome. *Lancet* **361**, 1773–1778 (2003).
10. Peiris, J.S. *et al.* Clinical progression and viral load in a community outbreak of coronavirus-associated SARS pneumonia: a prospective study. *Lancet* **361**, 1767–1772 (2003).
11. Bisht, H. *et al.* Severe acute respiratory syndrome coronavirus spike protein expressed by attenuated vaccinia virus protectiveloy immunizes mice. *Proc. Natl. Acad. Sci. USA* **101**, 6641–6646 (2004).
12. Bukreyev, A. *et al.* Mucosal immunization of African green monkeys (*Cercopithecus aethiops*) with an attenuated parainfluenza virus expressing the SARS coronavirus spike protein for the prevention of SARS. *Lancet* **363**, 2122–2127 (2004).
13. Yang, Z. *et al.* A DNA vaccine induces SARS coronavirus neutralization and protective immunity in mice. *Nature* **428**, 561–564 (2004).
14. Hogan, R. *et al.* Resolution of primary severe acute respiratory syndrome-associated coronavirus infection requires Stat1. *J. Virol.* **78**, 11416–11421 (2004).
15. Zhong, N.S. *et al.* Epidemiological and cause of severe acute respiratory syndrome (SARS) in Guangdong, People's Republic of China, in February, 2003. *Lancet* **362**, 1353–1358 (2004).
16. Subbarao, K. *et al.* Prior infection and passive transfer of neutralizing antibody prevent replication of severe acute respiratory syndrome coronavirus in the respiratory tract of mice. *J. Virol.* **78**, 3572–3577 (2004).
17. Hensley, L. *et al.* Interferon-β 1a and SARS coronavirus replication. *Emerg. Infect. Dis.* **10**, 317–319 (2004).
18. Sainz, B. Jr. *et al.* Interferon-beta and interferon-gamma synergistically inhibit the replication of severe acute respiratory syndrome-associated coronavirus (SARS-CoV). *Virology* **329**, 11–17 (2004).
19. Haagmans, B.L. *et al.* Pegylated interferon-α protects type 1 pneumocytes against SARS coronavirus infection in macaques. *Nat. Med.* **10**, 290–293 (2004).
20. Rowe, T. *et al.* Macaque model for severe acute respiratory syndrome. *J. Virol.* **78**, 11401–11404 (2004).
21. Chen, Z. *et al.* Recombinant modified vaccinia virus ankara expressing the spike glycoprotein of severe acute respiratory syndrome coronavirus induces protective neutralizing antibodies primarily targeting the receptor binding region. *J. Virol.* **79**, 2678–2688 (2005).
22. Qin, C. *et al.* An animal model of SARS produced by infection of macaca mulata with SARS coronavirus. *J. Pathol.* **206**, 251–259 (2005).
23. Joost Haasnoot, P.C.J., Cupac, D. & Berkhout, B. Inhibition of virus replication by RNA interference. *J. Biomed. Sci.* **10**, 607–616 (2003).
24. Zheng, B. *et al.* Prophylactic and therapeutic effects of small interfering RNA targeting SARS-coronavirus. *Antivir. Ther.* **9**, 365–374 (2004).

25. Elmen, J. *et al.* SARS virus inhibited by siRNA. *Preclinica.* **2**, 135–142 (2004).
26. Zhang, Y. *et al.* Silencing SARS-CoV protein expression in cultured cells by RNA interference. *FEBS Lett.* **560**, 141–146 (2004).
27. Zhang, R. *et al.* Inhibiting severe acute respiratory syndrome-associated coronavirus by small interfering RNA. *Chin. Med. J. (Engl.)* **116**, 1262–1264 (2003).
28. Wang, Z. *et al.* Inhibition of severe acute respiratory syndrome virus replication by small interfering RNAs in mammalian cells. *J. Virol.* **78**, 7523–7527 (2004).
29. Ghanayem, N.S. *et al.* Stability of dopamine and epinephrine solutions up to 84 hours. *Pediatr. Crit. Care Med.* **2**, 315–317 (2001).
30. Thomas, N.J. *et al.* Cost-effectiveness of exogenous surfactant therapy in pediatric patients with acute hypoxemic respiratory failure. *Pediatr. Crit. Care Med.* **6**, 160–165 (2005).
31. Lu, P.Y., Enist, D. & Mina, M. Method of achieving persistent transgene expression. US patent application. 20030148975, PCT/EP00/13297 (2000).
32. Massaro, D., Massaro, G.D. & Clerch, L.B. Noninvasive delivery of small inhibitory RNA and other reagents to pulmonary alveoli in mice. *Am. J. Physiol. Lung Cell. Mol. Physiol.* **287**, L1066–1070 (2004).
33. Bitko, V., Musiyenko, A., Shulyayeva, O. & Barik, S. Inhibition of respiratory viruses by nasally administered siRNA. *Nat. Med.* **11**, 50–55 (2004).
34. Tompkins, S.M., Lo, C.Y., Tumpey, T.M. & Epstein, S.L. Protection against lethal influenza virus challenge by RNA interference *in vivo*. *Proc. Natl. Acad. Sci. USA* **101**, 8682–8686 (2004).
35. Ge, Q. *et al.* Inhibition of influenza virus production in virus-infected mice by RNA interference. *Proc. Natl. Acad. Sci. USA* **101**, 8676–8681 (2004).
36. Boeckle, S. *et al.* Purification of polyethylenimine polyplexes highlights the role of free polycations in gene transfer. *J. Gene Med.* **6**, 1102–1111 (2004).
37. Delepine, P. *et al.* Biodistribution study of phosphonolipids: a class of non-viral vectors efficient in mice lung-directed gene transfer. *J. Gene Med.* **5**, 600–608 (2003).
38. Bonnard, E., Mazarguil, H. & Zajac, J.M. Peptide nucleic acids targeted to the mouse proNPFF(A) reveal an endogenous opioid tonus. *Peptides* **23**, 1107–1113 (2002).
39. Semizarov, D. *et al.* Specificity of short interfering RNA determined through gene expression signatures. *Proc. Natl. Acad. Sci. USA* **100**, 6347–6352 (2003).
40. Chi, J.T. *et al.* Genomewide view of gene silencing by small interfering RNAs. *Proc. Natl. Acad. Sci. USA* **100**, 6364–6369 (2003).
41. Jackson, A. *et al.* Expression profiling reveals off-target gene regulation by RNAi. *Nat. Biotechnol.* **21**, 635–637 (2003).
42. Sledz, C.A. *et al.* Activation of the interferon system by short-interfering RNAs. *Nat. Cell Biol.* **5**, 834–839 (2003).
43. Kariko, K., Bhuyan, P., Capodici, J. & Weissman, D. Small interfering RNAs mediate sequence-independent gene suppression and induce immune activation by signaling through toll-like receptor 3. *J. Immunol.* **172**, 6545–6549 (2004).
44. Judge, A.D. *et al.* Sequence-dependent stimulation of the mammalian innate immune response by synthetic siRNA. *Nat. Biotechnol.* **23**, 457–462 (2005).
45. Hornung, V. *et al.* Sequence-specific potent inductin of IFN-α by short interfering RNA in plasmacytoid dentritic cells through TLR7. *Nat. Med.* **11**, 263–70 (2005).
46. Heidel, J.D. *et al.* Lack of interferon response in animals to naked siRNAs. *Nat. Biotechnol.* **22**, 1579–1582 (2004).
47. Ware, L.B. & Matthay, M.A. The acute respiratory distress syndrome. *N. Engl. J. Med.* **342**, 1334–1349 (2000).
48. Yuen, K.Y. *et al.* Clinical features and rapid viral diagnosis of human disease associated with avian influenza A H5N1 virus. *Lancet* **351**, 467–471 (1998).
49. Huang, K.J. *et al.* An interferon-gamma-related cytokine storm in SARS patients. *J. Med. Virol.* **75**, 185–194 (2005).
50. Cinatl, J. *et al.* Treatment of SARS with human interferons. *Lancet* **362**, 293–294 (2003).